Journal of Molecular Catalysis A: Chemical 313 (2009) 38–43

Contents lists available at ScienceDirect

Journal of Molecular Catalysis A: Chemical

journal homepage: www.elsevier.com/locate/molcata

Promoting effect of Mg in supported Mo/HBeta–Al_2O_3 catalyst for cross-metathesis of ethene and butene-2 to propene

Xiujie Li, Weiping Zhang*, Shenglin Liu, Sujuan Xie, Xiangxue Zhu, Xinhe Bao, Longya Xu*

State Key Laboratory of Catalysis, Dalian Institute of Chemical Physics, Chinese Academy of Sciences, 457 Zhongshan Road, Dalian 116023, China

ARTICLE INFO

Article history:
Received 16 April 2009
Received in revised form 23 June 2009
Accepted 24 July 2009
Available online 3 August 2009

Keywords:
Propene
Olefin metathesis
Mo/HBeta–Al_2O_3 catalyst
Mg
Promoting effect

ABSTRACT

Promoting effects of Mg in heterogeneous Mo/HBeta–Al_2O_3 catalyst have been carefully studied for cross-metathesis of ethene and butene-2 to propene. The catalyst shows good stability with Mg content in the range of 1–2 wt%. Such effect may be attributed to the elimination of weak acid sites through introduction of Mg which suppresses the side olefin oligomerization reaction, as evidenced from NH_3-TPD and ^1H MAS NMR results. Addition of more Mg content to 3 wt% may change the state and reducibility of Mo species, as indicated from the UV–vis, UV-Raman and H_2-TPR measurements. The increasing difficulty for the reduction of Mo(VI) species is closely related with the poor performance of 3 wt% Mg–4Mo/HBeta–30% Al_2O_3 catalyst in the metathesis reaction.

1. Introduction

Propene is one of the most important basic petrochemicals as a raw material for the production of polypropene, polyacrylonitrile, acrolein and acrylic acid. In nowadays, the demand for propene is growing rapidly in worldwide chemical market. Olefin metathesis reaction provides an alternative route to produce propene. Olefin Conversion Technology (OCT) based on WO_3/SiO_2 catalyst has been industrialized by ABB Lummus Global [1]. Recently our laboratory reported a study of Mo supported on HBeta–Al_2O_3 composite support and it exhibited high activity in the metathesis reaction of ethene and butene-2 to propene at relative low temperature [2]. However, for further application in industry the stability of the catalyst needs to be well understood and improved. Studies on the effect of alkali metal additives to heterogeneous olefin metathesis catalysts on their performance in metathesis reactions have been reported elsewhere [3–5]. Introduction of sodium or magnesium to oxide systems, in particular to silica-supported tungsten catalysts, has a beneficial effect on the metathesis activity of propene. However, explanation of the effect of additives on a molecular scale has not been reported yet. Here magnesium oxide is used as an additive in our previous optimized catalyst of 4.0 wt% Mo supported on a composite support of 70% HBeta zeolite and 30% Al_2O_3, and much attention has been paid to its influence on the metathesis activity and stability [6]. NH_3-TPD and ^1H MAS NMR were applied to detect the acidity change. State of Mg species and its influence on Mo were further investigated by H_2-TPR, UV–vis and UV-Raman measurements. The promoting effect of Mg in the supported Mo/HBeta–Al_2O_3 catalyst was revealed by correlating the characterization results with the catalyst performances in cross-metathesis of ethene and butene-2 to propene.

2. Experimental

2.1. Catalyst preparation and evaluation

The HBeta and γ-Al_2O_3 composite support was prepared by extruding a mixture of γ-Al_2O_3 and HBeta zeolite (Si/Al = 15 provided by Fushun Petroleum Company, China) powder into strips with a diameter of about 2 mm. The support was designed as HB–30Al, which meant the weight percent of alumina in the support was 30%. The composite support was ground into 16–32 meshes after calcination at 500 °C for 2 h. Catalysts with Mo loading were prepared by wet impregnation of HB–30Al strips with an aqueous solution of $(NH_4)_6Mo_7O_{24}{\cdot}4H_2O$, then dried at 120 °C and finally calcined at 680 °C for 2 h. The catalysts were denoted as 4Mo/HB–30Al, where 4 (%) stood for the weight percent of Mo atoms in the catalysts when preparation. In the case of Mg loading, 4Mo/HB–30Al catalysts were impregnated to incipient wetness with Mg $(NO_3)_2$ solution to give the desired Mg content. Subse-

* Corresponding authors. Tel.: +86 411 8437 9279; fax: +86 411 8469 3292.
E-mail addresses: wpzhang@dicp.ac.cn (W. Zhang), lyxu@dicp.ac.cn (L. Xu).

1381-1169/$ – see front matter © 2009 Elsevier B.V. All rights reserved.
doi:10.1016/j.molcata.2009.07.020

quently, the catalysts were dried at 120 °C for 4 h before calcination at 500 °C for 2 h and designed as *n*Mg–4Mo/HB–30Al where *n* (%) represented the weight percent of Mg in the catalyst.

The catalysts (2.0 g) were tested in a fixed-bed up-flow stainless reactor of 10 mm in diameter with quartz sand to fix the catalyst bed. Quartz wool was applied to separate the catalyst from the quartz sand. In the middle of catalyst bed, a thermocouple was applied to detect the reaction temperature. Two pieces of controlling temperature thermocouple were set at the half-upper and half-bottom of the furnace, respectively. Such arrangement ensured that the constant temperature region was wider than the catalyst bed length (50 mm).

After activation for 1 h at 550 °C under nitrogen to remove the moisture, they were cooled down to the reaction temperature at 120 °C. The reaction products were analyzed by a Varian CP/3800 gas chromatograph equipped with alumina-plot column and an FID detector. Ethene feed (>99.9) was obtained from Dalian Special Gas Company and butene-2 (butene-2 65%, butane 35%) as cracking product was provided by Sinopec Qilu Company Ltd. The conversion of butene-2 was calculated on the basis of carbon number using butane as the internal standard. In the metathesis reaction of ethene and butene-2, propene was the main product. Trace amounts of butene-1 and C_5–C_7 oligomers were also detected in the product. Propene selectivity represented the propene weight percent in the gas products. Carbonaceous deposits on catalyst were not taken into account for the calculation.

2.2. XRD measurements

X-ray diffraction patterns were obtained at room temperature on a Rigaku D/Max-RB diffractometer using Cu Kα radiation. Powder diffractograms of samples were recorded over a range of 2θ values from 5–50° under the conditions of 40 kV and 100 mA at a scanning rate of 8°/min.

2.3. NH_3-TPD and H_2-TPR measurements

Temperature-programmed desorption of ammonium (NH_3-TPD) measurements were carried out in a conventional U-shaped stainless-steel micro-reactor (i.d. = 4 mm) using flowing helium (He) as the carrier gas. The NH_3-TPD process was monitored by an on line gas chromatograph (Shimadzu GC-8A) equipped with a TCD detector. Typically 140 mg sample was pretreated at 600 °C for 1 h in flowing He (25 ml/min), then cooled to 150 °C and saturated with NH_3 gas. After that, the sample was purged with pure He stream for certain time until a stable GC-baseline was attained. Subsequently NH_3-TPD experiment was carried out in the range of 150–600 °C at a heating rate of 18.8 °C/min.

Temperature-programmed reduction (TPR) experiments under H_2 were carried out in a conventional setup connected with different gases for the pretreatment of the sample, with a gas chromatography as the H_2 detector. The catalyst (about 80 mg) was put in a tubular quartz reactor. Under flowing 10% H_2/Ar flow (20 ml/min), H_2-TPR profiles were obtained in the range of 50–800 °C at a heating rate of 14 °C/min after the sample had been pretreated in an Ar flow at 500 °C for 60 min.

2.4. ^1H MAS NMR experiments

^1H MAS NMR spectra were recorded on a Varian Infinityplus-400 spectrometer equipped with a 4 mm probe. Before the ^1H MAS NMR measurements, samples were dehydrated at 400 °C under a pressure below 10^{-2} Pa for 20 h. Then ^1H MAS NMR spectra were collected at 399.9 MHz using single-pulse sequence with $\pi/4$ pulse, 4 s recycle delay with a spinning speed of 10 kHz. Chemical shifts were referenced to DSS. For the determination of quantitative results, all samples were weighed, and the spectra were calibrated by measuring a known amount of 1,1,1,3,3,3-hexafluoro-2-propanol performed in the same conditions [6].

2.5. UV–vis and UV-Raman measurements

UV–vis spectra of samples were recorded in a diffuse reflectance mode with a JASCO V-550 spectrometer at room temperature in the range of 190–600 nm at a rate of 40 nm/min.

UV-Raman spectra were recorded on a home-assembled UV-Raman spectrograph using a Jobin-Yvon T64000 triple-stage spectrograph with spectral resolution of 2 cm^{-1}. The laser line at 325 nm of a He–Cd laser was used as an exciting source with an output of 50 mW. The power of the laser at samples was about 1.0 mW. The 244 nm line from a Coherent Innova 300 Fred laser was used as another excitation source. The power of the 244 nm line at samples was below 1.0 mW.

3. Results and discussions

3.1. Metathesis activities of nMg–4Mo/HB–30Al catalysts

Metathesis activities of 4Mo/HB–30Al catalyst and the influence of Mg loadings were carefully investigated and shown in Fig. 1. For the 4Mo/HB–30Al catalyst, initial butene-2 conversion is high to 80% and it is stable during the first 4 h. The catalytic performance is a little lower than what we reported before due to the different sets of butene-2 feed [6]. According to dynamics equilibrium calculation, the maxima butene-2 conversion is 85.4% at 120 °C under 1 MPa. For 4Mo/HB–30Al catalyst, the butene-2 conversion is near to equilibrium value. When the time on stream is longer than 5 h, butene-2 conversion decreases gradually and it becomes only 73% at the time of 9 h. Product selectivity for propene is always stable and higher than 95%. Introduction of Mg into the catalyst has a promoting effect on the metathesis activity of the 4Mo/HB–30Al catalyst. When the Mg loading is 1%, butene-2 conversion is a little higher than that of 4Mo/HB–30Al. At the same time 1Mg–4Mo/HB–30Al shows better stability than that of 4Mo/HB–30Al although it also declines slightly with time. As the content of Mg increases to 2%, 2Mg–4Mo/HB–30Al catalyst exhibits an induction period of 3 h. After that, butene-2 conversion remains above 80% even after on stream for 9 h. Such break-in phenomena have also been observed on Mo or W based catalysts supported on SiO_2 in the metathesis reaction of propene [7–9]. Detailed studies about induction period

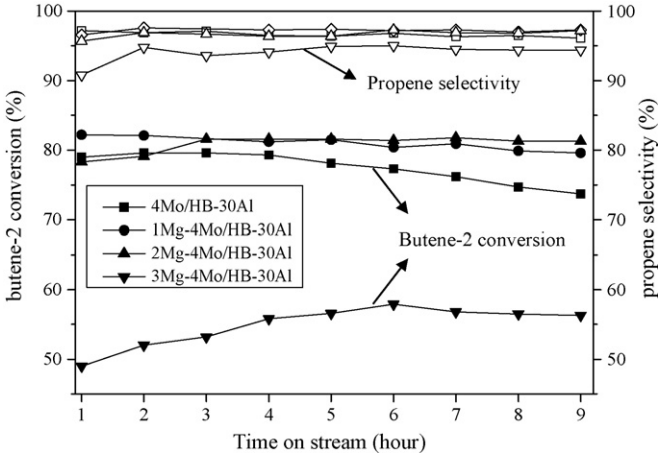

Fig. 1. Influences of Mg loading on the metathesis activity of 4Mo/HB–30Al catalysts. Filled symbols represent butene-2 conversion and open symbols represent propene selectivity (reaction temperature: 120 °C, pressure: 1.0 MPa, ethene/butene-2 = 3/1, WHSV of ethene: 1.2 h^{-1}).

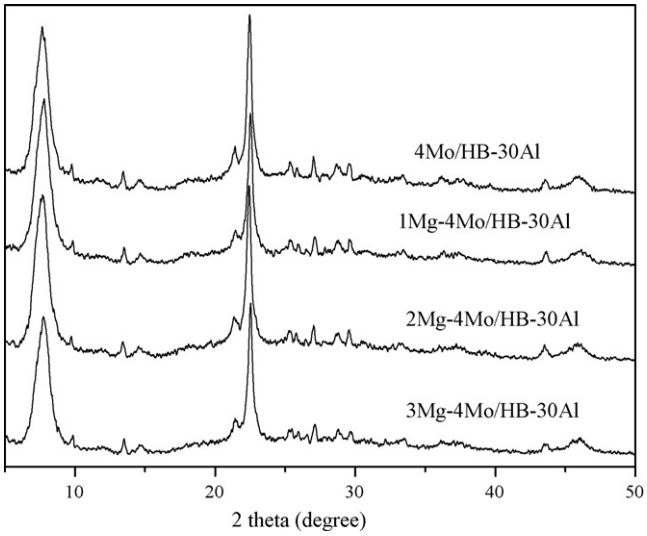

Fig. 2. XRD patterns of 4Mo/HB–30Al catalysts with different Mg loadings.

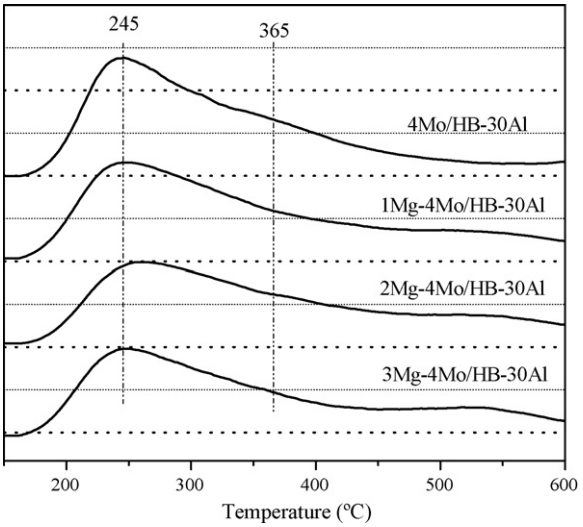

Fig. 3. NH_3-TPD profiles of 4Mo/HB–30Al catalysts with different Mg loadings.

on Mo based Mo/HBeta–Al_2O_3 catalyst are currently in progress. As far as 3Mg–4Mo/HB–30Al catalyst is concerned, initial butene-2 conversion drops sharply to 50%, indicating that high Mg content is not good for the metathesis reaction. Furthermore, a longer induction period of 6 h is observed before reaching the maximum activity, suggesting that induction period is related with the Mg loading of the catalyst under existing reaction conditions.

3.2. XRD patterns of 4Mo/HB–30Al catalysts with different Mg loadings

XRD patterns of the parent and Mg-modified catalysts are compared in Fig. 2. It is clear that the structure and the crystalline properties of HBeta zeolite remain unchanged with the modification of Mg when the Mg content is lower than 2%. For 3Mg–4Mo/HB–30Al sample, typical diffraction peak intensity of Beta zeolite at 7.6° and 22.4° decreases a little, which indicates that there exists interaction between Mg species and the support [10]. In addition, no crystalline MgO could be detected in the XRD spectra, suggesting that MgO has been highly dispersed on the surface of catalyst or the relatively low content of MgO is beyond the detection limit of XRD [11].

3.3. Acidity measurements of nMg–4Mo/HB–30Al catalysts

3.3.1. NH_3-TPD profiles of 4Mo/HB–30Al catalysts with different Mg loadings

In order to get more information about the acid sites before and after Mg loading, NH_3-TPD profiles are applied to monitor the acidity changes of the catalysts. As shown in Fig. 3, a main desorption peak centering at about 245 °C, as well as a shoulder peak 365 °C, could be differentiated for the 4Mo/HB–30Al sample. It is generally accepted that the peak at low temperature is linked with the weak acid sites of the catalyst mainly from alumina and the peak at high temperature is related with the strong acid sites from HBeta zeolite [12]. Further detailed assignments and interpretation of acid sites are limited due to the fact that both HBeta zeolite and Al_2O_3 are employed as supports. As shown in Fig. 3, the intensities of both desorption peaks, particularly the peak at low temperature, decrease with the introduction of Mg. This indicates that there are interactions between Mg species and the weak acid sites of the 4Mo/HB–30Al catalyst. Loss of weak acid sites may suppress the side reactions including olefin oligomerization to some degrees, which contributes to the good stability of Mg-modified metathesis catalysts [13]. For the 3Mg–4Mo/HB–30Al sample, high temperature peak intensity shows obvious decreasing trend. As the strong acid sites are contributed mainly from the Brønsted acid sites of the catalyst, loss of the strong acid sites becomes one of the important reasons leading to the lower metathesis activity [6,14]. Besides, a broad and weak desorption signal appears with the Mg loading. However, this peak could not be observed monitoring the fragment with m/e of 17 as representative of ammonia using mass spectrometer as detector. It may be related with the trace amounts of H_2O molecule interacting strongly with the zeolite framework.

3.3.2. ^1H MAS NMR spectra of 4Mo/HB–30Al catalysts with different Mg loadings

High-resolution ^1H MAS NMR is a useful and direct method to characterize the acid sites in zeolites and porous materials. Fig. 4 shows the ^1H MAS NMR spectra of 4Mo/HB–30Al catalysts with different Mg loadings. The signal at about 0.8 ppm is assigned to non-acidic unperturbed extra-framework aluminum hydroxyls. The peak at *ca.* 2.4 ppm may contain the contribution of non-framework Al–OH in HBeta zeolite and the acidic hydroxyls in alumina [14,15]. Due to the complexity of the support, different Al–OH in alumina ranging from 2.0 to 3.2 ppm may contribute to the signal at 2.4 ppm [16]. Additionally, another peak at 1.7 ppm could be observed, which is attributed to silanol groups in HBeta. At the same time the peak at 3.9 ppm could be clearly resolved and should

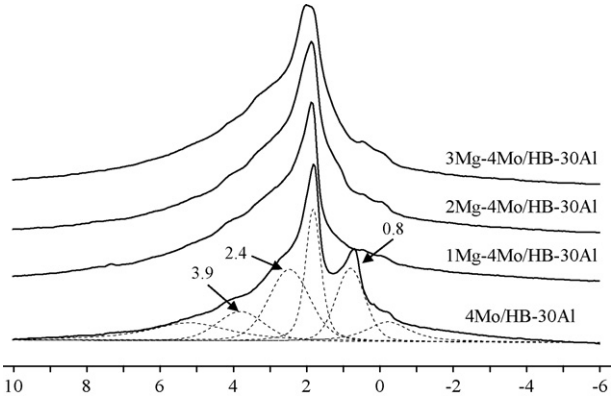

Fig. 4. ^1H MAS NMR spectra of 4Mo/HB–30Al catalysts with different Mg loadings. The spinning rate was 10 kHz, and 200 single-pulse scans were accumulated.

be assigned to the bridging hydroxyl groups, i.e., Brønsted acidic sites in HBeta. Fig. 4 shows that the total ^{1}H signal intensity does not decrease obviously with 1–2 wt% Mg loading. However, the peak at 0.8 ppm is preferentially reduced compared with that at 3.9 ppm. The amount of non-acidic unperturbed extra-framework Al–OH decreased from 235 to 45 μmol/g after introduction of 1% Mg. It can be deduced that during the preparation of catalysts Mg species first reacts with the non-acidic unperturbed extra-framework aluminum hydroxyls on the surface of the catalysts which is consistent with the NH_3-TPD results. Elimination of the extra-framework Al–OH with the introduction of appropriate Mg could improve the stability of 4Mo/HB–30Al catalyst in the olefin metathesis reaction. Due to the simultaneous consumption of the Brønsted (3.9 ppm) and acid Al–OH sites (2.4–3.0 ppm) after Mg introduction, there seems like a small shoulder peak appearing at 3.1 ppm. This signal could be associated with another type of non-framework Al–OH due to the complexity of the support [16]. When the Mg loading increases to 3%, the content of the Brønsted acidic sites decreases from original 151 to 95 μmol/g indicating Mg species interact with the framework Al and lead to the loss of bridging hydroxyl groups.

Introduction of 1–2% Mg to the 4Mo/HB–30Al catalyst may eliminate part of the weak acid sites on the catalyst evidenced by the NH_3-TPD results. This could be further proved by the ^{1}H MAS NMR experiments in which the non-acidic unperturbed extra-framework aluminum hydroxyls were preferentially consumed. As the oligomerization side reaction induced by the acid sites is directly related with deactivation of the catalyst, the suppression of the olefin oligomerization may contribute to the better stability of 1–2% Mg–4Mo/HB–30Al metathesis catalyst [13]. Increasing the Mg content to 3% further leads to the consumption of strong acid sites including Brønsted acidic sites as shown in Fig. 4. Not only the metathesis activity decreases, but also does the objective product propene selectivity. This is due to the increasing amounts of 1-butene in the product. In other words, relatively high content of Mg in the catalyst promotes the isomerization side reaction as magnesia is good isomerization catalyst [17].

3.4. Influences of Mg loading on the sate of Mo species on nMg–4Mo/HB–30Al catalyst

3.4.1. H_2-TPR profiles of 4Mo/HB–30Al catalysts with different Mg loadings

It is well accepted that olefin metathesis reaction follows metal carbene mechanism over heterogeneous catalysts [18]. Therefore, the forms of Mo species play an important role in the cross-metathesis of ethene and butene-2 to propene. Introduction of Mg to the catalyst may have influences on the existing state of Mo species. Here H_2-TPR and UV–vis techniques are applied to detect the state changes of Mo species upon Mg loading.

For the 4Mo/HB–30Al sample, three main reduction peaks locating at 475, 590, and 800 °C are observed as shown in Fig. 5. As reported in earlier literatures [19,20], reduction peak at 475 °C is related to the first step reduction of $Mo^{6+} \rightarrow Mo^{4+}$ of well dispersed octahedral Mo species. The peak at 800 °C is connected with the second step of reduction of octahedral Mo species and the first step of reduction of tetrahedral Mo species that are strongly bounded to the support. Considering the assignment of peak at 590 °C, Dora et al. [21] thought that it was a kind of polymeric Mo species linked with zeolite in the support. Its appearance was parallel with the increase content of zeolite in the support as they observed. However, on the SiO_2–Al_2O_3 support such a peak was also found by Marini and co-workers [20] and Prins and co-workers [22]. Therefore, we tentatively attribute this reduction peak to polymeric Mo species linked with Brønsted acid sites on the support. After introduction of 1% Mg to the catalyst, it could be clearly observed that the reduction peak at 475 °C shifts to higher temperatures. The incorporation of more Mg to the catalyst changes the state distribution of Mo species. The reduction peak at 475 °C corresponding to octahedral Mo species in 4Mo/HB–30Al shifts to 550 °C in 2Mg–4Mo/HB–30Al. Meanwhile, the peak of polymeric Mo species shifts from 590 to 610 °C. It is clear that Mo species in octahedral form are more and more difficult to be reduced upon Mg loading. When the Mg content is high to 3%, the first reduction peak becomes only a shoulder of polymeric Mo species reduction peak. This is directly related with the poor catalyst performance in the ethene and butene-2 to propene metathesis reaction.

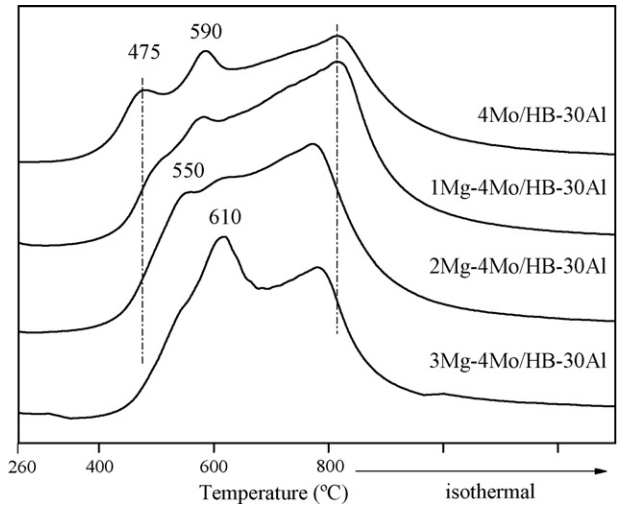

Fig. 5. H_2-TPR profiles of 4Mo/HB–30Al catalysts with different Mg loadings.

3.4.2. UV–vis and UV-Raman spectra of 4Mo/HB–30Al catalysts with different Mg loadings

Surrounding geometries of Mo species have great influences on the reduction peak positions. UV–vis spectra are applied in a diffuse reflectance mode and shown in Fig. 6. As Mg is incorporated to the 4Mo/HB–30Al catalysts, the absorption edge shifts to lower wavelength which indicates a decrease of octahedral Mo species and an increase of tetrahedral ones according to the assignments reported previously in the literature for alumina [23,24] and Mg supported Mo catalysts [25,26]. The observed changes in the Mo species with Mg content are in accordance with the H_2-TPR results. The growth in number of tetrahedral Mo species results in the higher temperature shift of the first reduction peak. Such phenom-

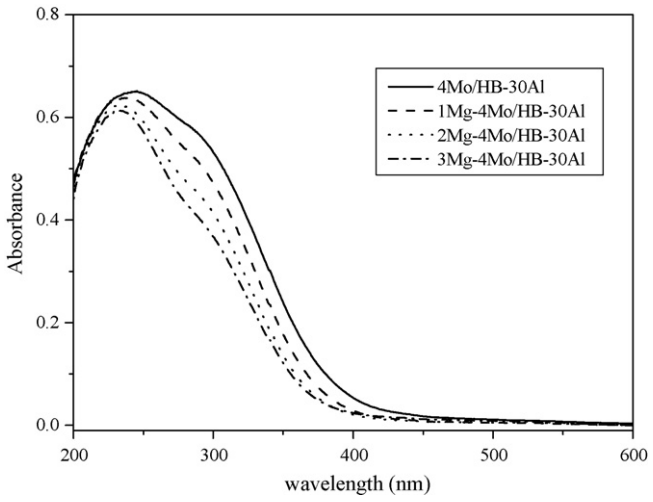

Fig. 6. UV–vis spectra of 4Mo/HB–30Al catalysts with different Mg loadings.

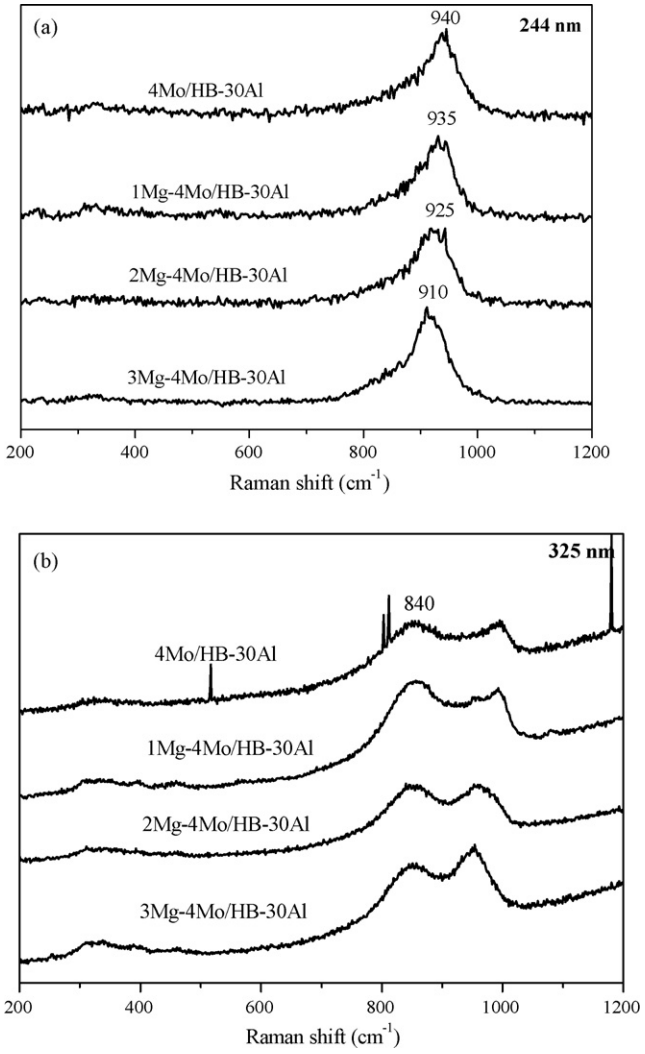

Fig. 7. UV-Raman spectra of 4Mo/HB–30Al catalysts with different Mg loadings using 244 nm (a) and 325 nm (b) laser lines as excitation sources.

ena have also been observed on MoO_3/MgO system by Llorente et al. [25].

To further distinguish the coordination structure of Mg modified 4Mo/HB–30Al catalysts, UV-Raman spectra with different enhancement bands of tetrahedral and octahedral species were applied to excite the electronic absorption of Mo species. The results are shown in Fig. 7. According to the UV–vis results, Mo=O bond of tetrahedral molybdate and Mo–O–Mo bridge bond of the octahedral species possess electronic absorptions at 220–240 and 320 nm, respectively. Thus, laser lines at 244 and 325 nm were chosen as the excitation sources to record the UV-Raman spectra [27].

UV-Raman spectra excited by 244 nm line exhibit Raman bands at 940 cm^{-1} for 4Mo/HB–30Al sample which is attributed to symmetric stretching mode of Mo=O bond of the tetrahedral molybdate [27–29]. Since the 244 nm line is located in the electronic absorption band of the tetrahedral Mo=O bond, resonance peak of Mo species in tetrahedral form is greatly enhanced. As the Mg loading increases from 0 to 3 wt%, the resonance band shifts from 940 to 910 cm^{-1}. As reported earlier [29,30], frequency of the band position is related with Mo=O bond length. The longer the terminal Mo=O band is, the lower the frequency for the band position is. Introduction of Mg leads to the changes of bond strength of Mo=O bond, which may be related with the reducibility of Mo species in H_2-TPR experiments. As shown in Fig. 5, the reduction peak of tetrahedral Mo species for 4Mo/HB–30Al sample locates at 800 °C. With Mg loading, this peak shifts to lower temperature, indicating that the tetrahedral Mo species can be reduced more easily. This may be correlated with the bond strength of terminal Mo=O bond evidenced by UV-Raman results. The shorter the Mo=O bond length is, the stronger the tetrahedral Mo species is.

As shown in Fig. 7(b), there are two dominant Raman bands at 840 and 970 cm^{-1} for 4Mo/HB–30Al excited by 325 nm line. Compared with the Raman spectra excited by 244 nm line, the new band at 840 cm^{-1} is assigned to the asymmetric stretching mode of the Mo–O–Mo bond of the octahedral species [27,29]. Obviously, this is enhanced because the 325 nm laser line accesses the electronic absorption of Mo–O–Mo bridge bond. An interesting phenomenon is that the relative line intensity of 840 and 970 cm^{-1} changes upon Mg loading. Ratios of Mo species in tetrahedral form increases with Mg content in the catalyst which is in agreement with the UV–vis spectra results. The growth in number of tetrahedral Mo species is parallel with the Mg content in the catalysts. This is also in consistent with the H_2-TPR results as Mo species in tetrahedral form are more difficult to be reduced compared with that in octahedral form.

It is well known that reducibility and state of Mo species are closely related with the metathesis activity of the catalyst. Many studies have been done to reveal the relations between the optimal valences of Mo species and the metathesis activity [9,31–34]. However, no common views have been accepted up to now due to the complexity of different reaction systems. In our case, the reaction temperature (120 °C) is relatively low and Mo species with lower valence are difficult to be obtained under olefin atmosphere. Mo^{5+} is supposed to be the most promising active precursors on the 4Mo/HB–30Al catalyst for ethene and butene-2 to propene. This could be further proved by the previous XPS results which showed that the Mo(IV) signals was present after long time on stream (14 h) accompanied by the deactivation of the catalysts [35]. Incorporation of Mg species leads to state change of Mo species from octahedral to tetrahedral form and the corresponding increasing reduction difficulty of Mo species evidenced by the higher temperature shift of the reduction peak in TPR results. It could be deduced that more time on stream under the olefin atmosphere is needed for Mo species to experience reduction. This may be a good explanation for the existence of long induction period on Mg containing catalysts. When Mg loading is high to 3%, the first reduction peak shifts to high reduction temperature accompanied with the lower metathesis activity of the catalyst. The increasing reduction difficulty of Mo species is an important factor resulting in the lower metathesis reaction activity on the 3Mg–4Mo/HB–30Al catalyst.

On basis of the above characterizations, promoting effect of Mg additive to the Mo/HBeta–Al_2O_3 catalyst could be explained clearly. Introduction of low content of Mg (<2%) may decrease the amount of weak acid sites on the catalyst, especially extra-framework aluminum hydroxyls, as evidenced by ^{1}H MAS NMR spectra. The elimination of weak acid sites may suppress the side oligomerization reactions and contribute to the better stability of the catalysts. Deduced from the UV-Raman and H_2-TPR results, when the Mg content is high to 3%, part of Mo species changes from octahedral to tetrahedral form, which increases the reduction difficulty of active Mo species and leads to the poor metathesis performances of 3Mg–4Mo/HB–30Al catalyst.

4. Conclusions

Catalytic performances of 4Mo/HBeta–30% Al_2O_3 catalysts with different Mg loadings were evaluated in detail. Addition of 1–2 wt% Mg loading, i.e., 1–2Mg–4Mo/HB–30Al catalyst, shows much better stability compared with the catalyst without Mg in the metathesis reaction of ethene and butene-2 to propene. NH_3-TPD and ^{1}H

MAS NMR results demonstrate that addition of Mg to the catalyst could eliminate the weak acid sites on the catalyst. This suppresses the side olefin oligomerization reactions, and improves the catalyst stability on stream. Addition of Mg loading up to 3 wt% not only decreases the acid sites but also changes the state of Mo species as evidenced by UV-Raman spectra. Increasing difficulty for Mo reduction may lead to the poor performance of the 3Mg–4Mo/HB–30Al catalyst.

Acknowledgments

We are grateful for the financial support of the National Natural Science Foundation of China (Grant nos. 20403017 and 20773120) and the Ministry of Science and Technology of China through the National Key Project of Fundamental Research (Grant nos. 2009CB623501 and 2009CB623507).

References

[1] J.C. Mol, J. Mol. Catal. A: Chem. 213 (2004) 39.
[2] S.L. Liu, S.J. Huang, W.J. Xin, J. Bai, S.J. Xie, L.Y. Xu, Catal. Today 93–95 (2004) 471.
[3] T. Kawai, H. Goto, Y. Yamazaki, T. Ishikawa, J. Mol. Catal. 46 (1988) 157.
[4] R.L. Banks, S.G. Kukes, J. Mol. Catal. 28 (1985) 117.
[5] R.L. Banks, Appl. Ind. Catal. 3 (1984) 215.
[6] X.J. Li, W.P. Zhang, S.L. Liu, L.Y. Xu, X.W. Han, X.H. Bao, J. Catal. 250 (2007) 55.
[7] A. Andreini, J.C. Mol, J. Colloid Interface Sci. 84 (1981) 57.
[8] J.C. Mol, A. Andreini, J. Mol. Catal. 46 (1988) 151.
[9] B. Zhang, Y. Li, Q. Lin, D. Jin, J. Mol. Catal. 46 (1988) 229.
[10] M.J. Eapen, K.S.N. Reddy, V.P. Shiralkar, Zeolites 14 (1994) 295.
[11] D. Mao, W. Yang, J. Xia, B. Zhang, Q. Song, Q. Chen, J. Catal. 230 (2005) 140.
[12] S.J. Huang, S.L. Liu, Q.J. Zhu, X.X. Zhu, W.J. Xin, H.J. Liu, Z.C. Feng, C. Li, S.J. Xie, Q.X. Wang, L.Y. Xu, Appl. Catal. A 323 (2007) 94.
[13] K.P. Datema, A.K. Nowak, J.V. Houckgeest, A.F.H. Wielers, Catal. Lett. 11 (1991) 267.
[14] X.J. Li, W.P. Zhang, S.L. Liu, L.Y. Xu, X.W. Han, X.H. Bao, J. Phys. Chem. C 112 (2008) 5955.
[15] X.J. Li, W.P. Zhang, S.L. Liu, L.Y. Xu, X.W. Han, X.H. Bao, J. Mol. Catal. A 250 (2006) 94.
[16] M. Hunger, Catal. Rev. - Sci. Eng. 39 (1997) 345.
[17] M.J. Baird, J.H. Lunsford, J. Catal. 26 (1972) 440.
[18] Y. Chauvin, Angew. Chem., Int. Ed. 45 (2006) 3740.
[19] R. Thomas, E.M. Van Oers, V.H.J. De Beer, J. Medema, J.A. Moulijn, J. Catal. 76 (1982) 241.
[20] S. Rajagopal, H.J. Marini, J.A. Marzari, R. Miranda, J. Catal. 147 (1994) 417.
[21] D. Solis, A.L. Agudo, J. Ramirez, T. Klimova, Catal. Today 116 (2006) 469.
[22] L. Qu, W.P. Zhang, P.J. Kooyman, R. Prins, J. Catal. 215 (2003).
[23] N. Giordano, J.C.J. Bart, A. Vaghi, A. Castellan, G. Martinotti, J. Catal. 36 (1975) 81.
[24] T. Klimova, D. Soli Casados, J. Ramiez, Catal. Today 43 (1998) 135.
[25] J.M. Llorente, V. Rives, P. Malet, F.J. Gil-Llambis, J. Catal. 135 (1992) 1.
[26] H. Aritani, T. Tanaka, T. Funabiki, S. Yoshida, K. Eda, N. Sotani, M. Kudo, S. Hasegawa, J. Phys. Chem. 100 (1996) 19495.
[27] G. Xiong, C. Li, Z. Feng, P. Ying, Q. Xin, J. Liu, J. Catal. 186 (1999) 234.
[28] C.C. Williams, J.G. Ekerdt, J.M. Jehng, F.D. Hardcastle, A.M. Turek, I.E. Wachs, J. Phys. Chem. 95 (1991) 8781.
[29] C.C. Williams, J.G. Ekerdt, J.M. Jehng, F.D. Hardcastle, I.E. Wachs, J. Phys. Chem. 95 (1991) 8791.
[30] F.D. Hardcastle, I.E. Wachs, J. Raman Spectrosc. 21 (1990) 683.
[31] W. Grunert, R. Feldhaus, K. Anders, E.S. Shpiro, K.M. Minachev, J. Catal. 120 (1989) 444.
[32] W. Grunert, A.Y. Stakheev, R. Feldhaus, K. Anders, E.S. Shpiro, K.M. Minachev, J. Catal. 135 (1992) 287.
[33] Y. Iwasawa, H. Ichinose, S. Ogasawara, M. Soma, J. Chem. Soc., Faraday Trans. 77 (1981) 1763.
[34] Y. Iwasawa, S. Ogasawara, J. Chem. Soc., Faraday Trans. 75 (1979) 1465.
[35] X.J. Li, W.P. Zhang, X. Li, S.L. Liu, H.J. Huang, L.Y. Xu, X.W. Han, X.H. Bao, J. Phy. Chem. C 113 (2009) 8228.